Origin and fate of Vanadium in the Hazeltine Creek Catchment following the 2014 Mount Polley mine tailings spill, British Columbia, Canada

Karen A. Hudson-Edwards[1], Patrick Byrne[2], Graham Bird[3], Paul A. Brewer[4], Ian T. Burke[5], Heather E. Jamieson[6], Mark G. Macklin[7], Richard D. Williams[8]*

[1] Environment & Sustainability Institute and Camborne School of Mines, University of Exeter, Penryn, Cornwall TR10 9FE, UK. *Corresponding author. Email k.hudson-edwards@exeter.ac.uk; Tel: +44-(0)1326-259-489.

[2] School of Natural Sciences and Psychology, Liverpool John Moores University, Liverpool, L3 3AF, UK. Email p.a.byrne@ljmu.ac.uk

[3] School of Environment, Natural Resources and Geography, Bangor University, Bangor, Gwynedd, LL57 2UW, UK. Email: g.bird@bangor.ac.uk

[4] Department of Geography and Earth Sciences, Aberystwyth University, Penglais, Aberystwyth, Ceredigion WY23 3FL, UK. pqb@aber.ac.uk

[5] School of Earth and Environment, University of Leeds, Leeds LS2 9JT, UK. i.t.burke@leeds.ac.uk

[6] Department of Geological Sciences and Geological Engineering, Queen's University, Kingston, Ontario K7L 3N6, Canada. jamieson@queensu.ca

[7] Lincoln Centre for Water and Planetary Health, School of Geography, College of Science, University of Lincoln, Brayford Pool, Lincoln, Lincolnshire LN6 7TS, UK. mmacklin@lincoln.ac.uk

[8] School of Geographical and Earth Sciences, University of Glasgow, Glasgow G12 8QQ, UK. Richard.Williams@glasgow.ac.uk

Submitted to: *Environmental Science & Technology*

Accepted: 4 March 2019

Keywords: Vanadium; Mount Polley; tailings; magnetite; titanite; XANES

ABSTRACT

Results are presented from the analysis of aqueous and solid-phase V speciation within samples collected from the Hazeltine Creek catchment affected by the August 2014 Mount Polley mine tailings dam failure, Canada. Electron microprobe and XANES analysis found that V is present as V^{3+} substituted into magnetite, and V^{3+} and V^{4+} substituted into titanite, both of which occur in the spilled Mount Polley tailings. Secondary Fe oxyhydroxides forming in inflow waters and on creek beds have V K-edge XANES spectra exhibiting E½ positions and pre-edge features consistent with the presence of V^{5+} species, suggesting sorption of this species on these secondary phases. PHREEQC modelling suggests that the stream waters mostly contain V^{5+}, and the inflow and pore waters contain a mixture of V^{3+} and V^{5+}. These data, and stream, inflow and pore water chemical data, suggest that dissolution of V(III)-bearing magnetite, V(III,IV)-bearing titanite, V(V)-bearing Fe(-Al-Si-Mn) oxhydroxides, V-bearing $Al(OH)_3$ and/or -clay minerals may have occurred. In the circumneutral pH environment of Hazeltine Creek elevated V concentrations are likely naturally attenuated by formation of V(V)-bearing secondary Fe oxyhydroxide, $Al(OH)_3$ or clay mineral colloids, suggesting that the V is not bioavailable. A conceptual model is presented describing the origin and fate of V in Hazeltine Creek that is applicable to other river systems.

ToC Art

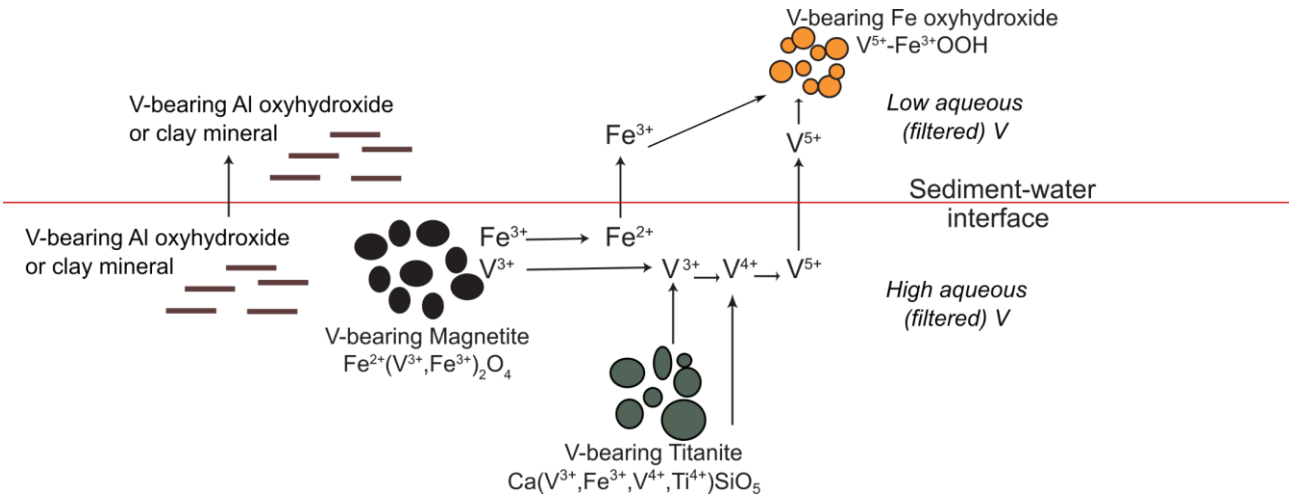
V-bearing Fe oxyhydroxide
V5+-Fe3+OOH
Low aqueous
(filtered) V
V-bearing Al oxyhydroxide
or clay mineral
Fe3+
V5+
Sediment-water
interface
V-bearing Al oxyhydroxide
or clay mineral
Fe3+
Fe2+
V3+
V3+
V4+
V5+
High aqueous
(filtered) V
V-bearing Magnetite
Fe2+(V3+,Fe3+)2O4
V-bearing Titanite
Ca(V3+,Fe3+,V4+,Ti4+)SiO5

INTRODUCTION

Vanadium (V) is a transition metal which is the 22nd most abundant in the Earth's crust[1,2] and occurs naturally in four oxidation states (V(II), V(III), V(IV) and V(V)). Although V is an essential element for humans and animals at low concentrations[3], intake of high concentrations of V can be carcinogenic and toxic[4,5]. Generally V(V) is considered to be the most toxic of the V species because it can inhibit or replace phosphate[6,7]. Vanadium is classed by the United Nations, US Environmental Protection Agency and Chinese Ministry of Environmental Protection as a priority environmental risk element[2,8,9,10]. In recognition of the potential toxicity of V, Canada has set a Federal Water Quality Guideline of 120 µg/L for protection of aquatic life in freshwater[11], and Schiffer and Liber[12] have suggested a more stringent chronic hazardous concentrations endangering only 5% of species (HC5) of 50 µg/L for Canadian freshwater organisms.

Humans can be exposed to vanadium mainly through inhalation and ingestion, potentially causing long-term respiratory and digestive problems, respectively[13]. Aqueous vanadate (V(V)) can also be taken up in benthic organisms such as *Hyalella azteca*[14], and have been shown to cause genotoxic and cytotoxic effects in higher plants[15]. Vanadium can be distributed in water, soil, sediment and air through the weathering of natural materials and through releases from anthropogenic activities including the burning of fossil fuels, application of pesticides and phosphate fertilizers, steel, aerospace and other industries, and mining[9,16,17]. For example, mining activities have led to contamination of waters and soils with V (e.g., 76-208 µg/L in groundwaters and 149 to 4800 mg/kg V in soils of the Panzhihua mining and smelting area, China[18,19]). There is, however, a lack of information on, and understanding of, the geochemical-mineralogical cycling of V in mining-affected environments[20], but these are required to determine health effects and to develop management and remediation schemes.

Mine tailings dam failures can rapidly add large amounts of V-bearing solid and liquid wastes to the fluvial environment[21]. Globally, failures of mine tailings dams impact significantly in the short- (hours to months) and long-term (years to centuries) on ecosystems and humans that live in affected

catchments, through erosion, deposition of tailings sediment and fluids, contamination of soil and water with potentially toxic metal and metalloid elements, and loss of life[22,23]. The 4th August 2014 failure of the tailings storage facility (TSF) at Mount Polley, British Columbia, Canada, is the second-largest by volume on record[23]. Approximately 25 Mm^3 of material, comprising 7.3 Mm^3 of tailings solids, 10.6 Mm^3 of supernatant water, 6.5 Mm^3 interstitial water and 0.6 Mm^3 of, tailings dam construction materials were discharged into the Quesnel River Watershed[23-25]. The material flowed north into and plugged Polley Lake, then was diverted south-east into Hazeltine Creek for 9.5 km. A significant proportion of the tailings and interstitial water (18.6 ± 1.4 M m^3; [25]) and eroded soils and vegetation[26] were deposited into the West Basin of Quesnel Lake (Figure 1). Deposition of tailings (average 1 m thick, but up to 3.5 m thick in the upper part of the area nearest the TSF) also occurred within the Hazeltine Creek catchment up to 100 m from the channel, especially near Polley Lake and Lower Hazeltine Creek[25]. Extensive clean-up has been undertaken since the spill (and since the sampling for this study was undertaken), comprising removal of most of the spilled tailings from, and restoration of, the catchment. This was aimed at restoring ecosystem habitats through the establishment of a new rock-lined channel, reducing remobilization of the remaining tailings and exposed natural sediments and decreasing turbidity[,27,28].

Mount Polley is a Cu-Au porphyry deposit, and the tailings comprise mostly silicate minerals (feldspars, ferro-magnesian and Ca-Ti-silicates, muscovite), oxides such as magnetite and rutile, carbonates, Cu sulfides and pyrite. Although the Mount Polley tailings have low sulfide (0.1 – 0.3 wt. %) and trace metal and metalloid concentrations[29] relative to other tailings[22,30,31], they have elevated concentrations of V (86 – 295 mg/kg) compared to local background soils (40.2 – 133 mg/kg[26]). Vanadium was also initially identified, in addition to Cu, Se and Mo, as a contaminant of potential concern in Hazeltine Creek soils[32]. The cycling of Cu in Hazeltine Creek has been previously examined in detail[26,29,33-37], but detailed geochemical and mineralogical studies of V, Se and Mo have not been conducted.

In this paper we focus on V due to its high environmental risk potential[2,8,9,10] and to the relative lack of data on its behavior in mining-affected environments[20]. We aim to understand the geochemical cycling of V in the Hazeltine Creek catchment and its implications for the origin, transport, fate and potentially toxicity of V in other river systems. The objectives of the study are to determine (1) V concentrations and speciation in stream, inflow and pore waters using aqueous composition data and PHREEQC modeling, (2) solid-phase V concentrations and speciation in the deposited tailings and secondary Fe oxyhydroxides using electron microprobe, automated mineralogy analysis and X-ray absorption spectroscopy (XAS) analysis, (3) the environmental origin, fate and potential hazard of the deposition of V-bearing tailings in mining-affected catchments following tailings dam failures and remediation. We present, for the first time to our knowledge for natural systems, evidence that dissolution of V-bearing magnetite and titanite may contribute to aqueous V. The results will also inform restoration and management schemes for river systems receiving V from other natural and anthropogenic sources.

MATERIALS AND METHODS

Field Site. The Mount Polley porphyry Cu-Au mine[38] is located in British Columbia, Canada, 275 km south-east of Prince George (Figure 1). Hazeltine Creek drains an area of 112 km^2, including Polley Lake (Figure 1), and flows 9.5 km in a south-easterly direction before discharging into Quesnel Lake. Hazeltine Creek has an alkaline pH (average 8.2 prior to the spill[39]; 7.0-9.3 from 30th July to 2nd August 2015[37]). The catchment is underlain by Late Triassic alkali intrusions, including the porphyry Cu-Au orebody, and by Mesozoic basaltic and andesitic volcanics, and glaciofluvial and glaciolacustrine deposits[38].

Water Sampling, Analysis and Speciation-Solubility modelling. Details of water sampling analysis and quality control are presented in Byrne et al.[37] and are summarized briefly here. In August 2015 sample collection comprised from 10 stream waters from Hazeltine Creek, 12 inflow waters seeping from riparian tailings into the creek, and 3 stream channel pore water sites collected at 10

and 20 cm depth through deposited tailings, natural stream sediments and bank materials (using a 3/8" stainless steel piezometer and peristaltic pump). The piezometer design used in this study was developed by the U.S. Geological Survey and has been used extensively to sample trace metals in pore waters. Standard practice for operating the piezometer is to flush with deionized water before and after pumping to ensure that the drive point itself is clean and not contaminated. Furthermore, it is unlikely that metal leaching would occur over the timescale of pore water pumping / sampling (2 – 3 min). Thus, we believe that there was no contribution of V or other metals to the pore water samples. The sampling took place when spilled tailings were being excavated and removed from the creek valley, creek turbidity was high and a new channel was being constructed. Thus, the results reported here could be considered to represent conditions that might be encountered during a spring freshet[34]. The concentrations of total and filtered (<0.45 µm) major (Al, Ca, K, Mg, Na, Si) and trace elements (As, Cd, Cu, Cr, Fe, Mo, Mn, Ni, Pb, Se, V, Zn) were determined by inductively coupled plasma – optical emission spectroscopy (Thermo Scientific iCAP 6500 Duo) and – mass spectroscopy (Thermo X-series 1), respectively. Ion chromatography (Dionex ICS-2500) was used to determine filtered anion (Cl, F, SO_4) concentrations Equilibrium modeling, using the measured aqueous concentrations and other aqueous parameters of the Hazeltine Creek stream, inflow and pore water samples, were carried out using the PHREEQC code and the minteq.dat.v4 thermodynamic database distributed with the code[40,41]. Alkalinity was estimated for the stream and inflow waters as bicarbonate by ion sum calculation (i.e., charge balanced was forced with bicarbonate). We carried out calculations to check if the modelled V speciation and saturation indices were sensitive to bicarbonate activity using different HCO_3 concentrations and found no significant differences in our results. Ferrihydrite and amorphous $Al(OH)_3$ were allowed to precipitate during the equilibrium modeling, as the waters are not likely to be very much oversaturated with respect to these minerals.

Tailings, Sediment and Fe oxyhydroxide Sampling and XRF V Analysis. In August 2016 samples of deposited tailings and a secondary Fe oxyhydroxide sample deposit scraped from a seep draining a re-profiled stream bank (Supplementary Table S4) were also collected in clean

polyethylene bags. These were air-dried and stored at 4 °C until used. A proportion was crushed and pressed into powder pellets for V analysis by XRF (Bruker S4 Pioneer). Sub-samples of deposited tailings (ST 09-02-01-140915 and WT 17-08-02-140912; Supplementary Table S4) collected in 2014 following the dam failure by consultants of Mount Polley Mining Corporation, and described in SNC-Lavalin Inc[26], were donated by the mine for comparison to samples collected by the authors.

Electron Microprobe and Automated Mineralogy Analysis. Polished blocks of all solid samples were examined with a Jeol 8100 Superprobe (WDS) with an Oxford Instrument Inca System (EDS). Spot analyses and X-ray chemical mapping were carried out by collecting energy data between 0 and 20 eV using a 15 kV accelerating voltage, 2.5 mA current and a spot size of 1 μm. The analyses were calibrated using a ZAF (atomic number, absorption, fluorescence) matrix correction with standards of oxides and Specpure metals. To quantify and further characterize and quantify the bulk mineralogy and those minerals identified with the Superprobe as containing V, the polished blocks were investigated using an Mineral Liberation Analysis automated mineralogy system on a FEI Quanta 650 FEG ESEM equipped with twin Bruker XFlash EDS detectors at Queen's University, Canada. Spectra were collected at 25kV, with a minimum of 2000 counts per analysis, collecting 250,000+ X-ray spectra on each sample to calculate total area percentages of each mineral detected, then a further 800,000 spectra at higher resolution searching and targeting V-bearing minerals at fine detail.

X-ray Absorption Spectroscopy (XAS) Analysis. Microfocus XANES V K-edge spectra (5465 eV) for individual magnetite, titanite and Fe oxyhydroxide grains were collected on beam line I18 at the Diamond Light Source operating at 3 GeV with a typical current of 300 mA, using a nitrogen cooled Si(111) double crystal monochromator and focusing optics. Kirkpatrick-Baez mirrors were used to produce a focused beam of 3 μm diameter at the sample. For samples and standards (V metal, V_2O_3, VO_2, V_2O_5, V(V) sorbed to FeOOH (see SI for preparation method)), K-edge spectra were collected in fluorescence mode at room temperature (~295 K) using a 4 element solid state Si detector. Because we analyzed V-bearing titanite we checked that the V Kα emission

line could be resolved, despite its overlap with the Ti Kβ emission line. On beamline I18, the Ti Kα emission at ~4510eV is resolvable in XRF detectors from the V Kα emission at ~4950 eV (250-300 eV separation is required for effective windowing of I18's XRF detectors). The lower intensity Ti K-β emission at 4932 eV is not resolvable by any XRF detector but the binding energy of the V-K edge (5465 eV) is about 500 eV above the Ti K-edge (4966 eV). Therefore, interference of the Ti K-β XAS spectra and V K-α XANES spectra was minimal and limited to long wavelength, low amplitude EXAFS oscillations, by 4950 eV Ti k-edge oscillations that would be not be apparent in V-XANES. After collecting the XANES data, multiple scans were then averaged to improve the signal to noise ratio using Athena version v0.8.061[42]. XANES spectra absorption data were also normalized in Athena over the full data range and plotted from approximately -15 eV to +30 eV relative to the edge position with no correction required for drift in E_0. Vanadium data were calibrated using E_0 measured from thin metal foils inserted downstream of the samples and measured simultaneously. The V-metal K-edge was detected and the E_0 position did not drift between spectra. The V pre-edge peak energy was determined by calculation of the area normalized centroid energy position (i.e., the peak intensity is normalized to the height of the main V K-edge step on the y-axis of the resultant graph, plotted against the area normalized pre-edge centroid peak energy position on the x-axis) following the method of Chaurand et al.[43], and used previously for solid-phase V speciation in bauxite residue[44].

RESULTS AND DISCUSSION

Aqueous V geochemistry and speciation. Filtered V concentrations (mean: 9 µg/L; range: 7 – 12 µg/L) in the Hazeltine Creek stream waters were slightly elevated compared to pre-event mean concentrations (1 µg/L[29]), higher than mean global filtered river concentrations (0.71 µg/L[45]), but lower than chronic hazardous concentrations recently identified for freshwater organisms[12].

Overall, filtered V concentrations declined with distance downstream of the Polley Lake weir (Figure 2). Filtered V concentrations in the stream waters were generally lower than those of the

inflows seeping from tailings (mean: 17 µg/L; range: 4 – 41 µg/L), but the inflow waters do not appear to have affected V concentrations downstream, likely because of their low volumes and flow rates (Figure 2). Unfiltered V concentrations in stream (mean: 15 µg/L; range: 11 – 21 µg/L) and inflow waters (mean: 59 µg/L; range: 4 – 303 µg/L[1]) were either similar to (within 7 µg/L; 62% of samples) or higher than (up to 278 µg/L; 38% of samples) their respective filtered concentrations[37]. Unfiltered V concentrations were highest in the inflow waters in the upper part of the catchment within approximately 2000 m of the Polley Lake weir (Figure 2).

Filtered V concentrations in the Hazeltine Creek stream waters at 0 cm in the sampled profiles (8 – 11 µg/L) were similar to those of the other stream waters collected. At 10 cm depth all filtered pore water V concentrations peaked (132, 1200 and 53 µg/L for PW-1, PW-2 and PW-3, respectively; Figure 3), but concentrations declined at 20 cm depth (83, 231 and 43 µg/L for PW-1, PW-2 and PW-3, respectively). Peaks in filtered V concentrations at 10 cm depth coincide with peaks in filtered Al, As, Ca, Cu, Fe, K, Mg, Mn, Ni, Zn and Si, and declines in ORP and pH (Figure 3). The fact that PW-2 has higher V concentrations than those in PW-1 and PW-3 might be due to its position at the downstream end of upper Hazeltine Creek (Figure 1), where the greatest amount of spilled tailings were deposited following the tailings dam failure, and still remained at the time of sampling in August 2015[37].

Filtered V concentrations for most of the pore waters are positively correlated with filtered concentrations of Fe, Al, Cr, Ni and Si, and slightly positive but flatter correlations with filtered Ca concentrations (Figure 4). By contrast, filtered concentrations of inflow waters are poorly correlated with Fe, Al and Ni, but show good correlations with Si, Ca and Cr, together with some of the pore water samples.

The PHREEQC modeling suggested that no minerals with V as a major component were oversaturated in any of the Hazeltine Creek waters (Supplementary Table S1). Calcite, diaspore and gibbsite were predicted to be slightly oversaturated in many of the samples (Supplementary Table S1). Pentavalent V was predicted to form 100% of all of the aqueous V species in all but one (HC9)

of the stream waters. By contrast, the inflow and pore waters are modeled to contain varying amounts of V(III) and V(V) (Supplementary Table S2. V(III) is modelled to dominate in some of the inflow waters and in the pore waters at 20 cm depth, and V(V) is predicted to dominate in the majority of the inflow waters and in the pore waters at 0 and 10 m depth (Supplementary Table S2). The modelling suggests that HVO_4^{2-} was the dominant species (50-86%) in all but one (HC9) of the stream waters, with lesser amounts of $H_2VO_4^-$ (14-50%; (Supplementary Table S3). The inflow and pore waters have relatively low calculated proportions of HVO_4^{2-} (inflow 23-63%, pore2146%) and relatively high proportions of $H_2VO_4^-$ (inflow 37-77%, pore 54-77%Supplementary Table S3). The highest V concentrations recorded in this study occur in inflow and pore waters with pH < 8.1-8.3, which is the equilibrium point between the weak acid and conjugate base (pKa) (pH 8.1 to 8.3) between HVO_4^{2-} and $H_2VO_4^-$ at 25°C[9,46].

We did not measure DOC concentrations and thus were not able to develop a V-organic complexation model. However, we acknowledge that V is known to bind with DOC in the form of humic acids and EDTA in aquatic environments[47,48,49] and therefore, that DOC may have played a role in V cycling in the Hazeltine Creek catchment.

Solid-phase V geochemistry and mineralogy. Concentrations of V in the study samples from 51 to 231 mg/kg (Supplementary Table S4), which are mostly within the range for Mount Polley tailings collected in 2014[26]. The V concentrations are lower than concentrations reported for some mine wastes (e.g. 860-963 mg/kg for red mud from the 2010 Ajka, Hungary, alumina processing repository failure[44]), but are within the same range as others (e.g., 135 mg/kg V for abandoned Au mine tailings, Nova Scotia, Canada[50]; 40.7 mg/kg V for polysulfide tailings, Boliden, Sweden[51]). The spilled tailings (samples POL-5- to 7, POL-9; Supplementary Table S5) are dominated by orthoclase and albite (both 32-41 area %), with lesser amounts of hornblende/augite (3.9-5.1 area %), epidote (3.5-4.9 area %), muscovite (3.2-3.8 area %), plagioclase (1.6-2.5 area %), quartz (1.3-2.4 area %) and chlorite (1.3-1.5 area %), similar to proportions found by Kennedy et al.[52]. Magnetite abundance is ascribed to Fe oxides in the automated mineralogy analysis, forming 1.2-3.1 area % of the total

mineralogy, while titanite forms 0.5-1.7 area %. A Cu-bearing Fe oxide phase containing >0.1 wt. % Cu was added to the automated mineralogy library[34], and this phase forms 0.5-2.3 area % of the tailings. The remaining samples (POL-12 to -14; Supplementary Table S5) contain higher proportions of quartz (20-50 area %), suggesting dilution by catchment soils.

Magnetite and titanite in the Mount Polley tailings both contain V (Figure 5), but no other tailings minerals were found to contain V at the detection limit of the microprobe (0.001 wt. %). Average V concentrations for 11 magnetite grains are 0.28 wt. % (range 0.16-0.37 wt. %), and for 14 titanite grains are 0.25 wt. % (0.14-0.35 wt. %). The latter are within the same order of magnitude to those determined by Celis[53] for 57 titanite grains from the Mount Polley deposit (mean 0.15 wt. % V, range 0.06-0.29 wt. % V). The magnetite also contain trace amounts of Si (mean 0.045 wt. %), and magnetite and titanite contain trace concentrations of Al (0.045 wt. % and 0.037 wt. %, respectively), Cr (0.042 wt. % and 0.001 wt. %, respectively) and Mn (0.13 wt. % and 0.042 wt. %, respectively). Vanadium concentrations in the Fe oxyhydroxide collected from a seep draining a re-profiled stream bank are low, at or below the limit of detection of the microprobe (≤ 0.001 wt. % V; 10 grains).

Vanadium XANES Analysis. Charaund et al.[43] proposed an elegant system for interpreting V K-edge XANES spectra based on the detail observation of pre-edge peak intensity and energy position. In this system, data are described in terms of variation in both co-ordination symmetry and valance state. Data are provided from multiple V(V) standards as V K-edge XANES is sensitive to changes in both valance and the mode of structural incorporation (e.g. V(V) on FeOOH is tetrahedral and V(V) in V_2O_5 is square pyramidal[54-56]). The multiple V(V) standards are therefore desirable in order to investigate the mode of V occurrence in samples. When the Mount Polly magnetite and titanite data are plotted in this scheme the sample data plots between the octahedral V^{3+} and V^{4+} standards. The magnetite samples appear to contain primarily V^{3+}, suggesting incorporation of V^{3+} via substitution for octahedral Fe^{3+} within the structure. This is consistent with other studies on magnetite[57-59], although Balan et al.[58] also found minor (<10 %) V(IV) occupying octahedral sites. The Mount Polley titanite V plots between octahedrally co-ordinated V^{3+} and V^{4+}

(Figure 6), suggesting that it most likely substituting for octahedrally co-ordinated Fe^{3+}, Al^{3+} or Ti^{4+} in the mineral structure. Celis[53] found that Mount Polley titanite contained almost equal concentrations of Al and Fe, substantiating the possibility of V^{3+} substitution for Fe^{3+} and Al^{3+}. Pan and Fleet[60] also reported that octahedrally co-ordinated V^{3+} and V^{4+} had similar radii to octahedrally co-ordinated Al^{3+} (0.64, 0.58, 0.535 Å, respectively[61]) and could therefore substitute for the latter within the vanadian titanite of the Hemlo gold deposit.

The V-bearing iron oxyhydroxide sample plots between V^{4+} (O_h) and the V^{5+} absorbed to FeOOH standards. It is possible that V in these samples is present as a mixture between the primary V^{4+} and V^{5+} in absorption complexes on hydrous iron oxyhydroxides. However, adsorbed V^{4+} does not persist in oxygenated environments as it is readily oxidized to V^{5+} [62], and most of the scientific literature reports the strong affinity of Fe oxyhydroxides such as goethite and ferrihydrite to V^{5+} [54,64,65]. Kaur et al.[65] attempted to make samples of V(III)-containing goethite, but found that some oxidation occurred, and that V(III), V(IV) and V(V) were also present. The resultant XANES spectra are intermediate between V(III) and V(V), similar to our spectra (Figure 6). Kaur et al.[65] also provided data that suggested that oxidized V was not readily incorporated in the goethite, and therefore are likely resent as adsorbed V(V) that was more easily removed by protons than more reduced forms.

Vanadium Cycling in Hazeltine Creek Following the Mount Polley Tailings Dam Failure and Remediation. V(III)-bearing magnetite and V(III) and/or V(IV)-bearing titanite (Figure 5, 6) were deposited within remobilized tailings and together with a large number of uprooted trees in the Hazeltine Creek catchment following the 2014 Mount Polley dam failure. It is also possible that lesser amounts of these minerals occurred within Hazeltine Creek channel and floodplain sediments and soils prior to the failure, given the relatively high V concentrations of some background soils[26]. A year after the tailings dam failure high filtered concentrations of V in pore waters occurring at 20 cm and especially 10 cm depth in Hazeltine Creek, coincide with peak concentrations in Al, As, Ca, Cu, Fe, K, Mg, Mn, Ni, Zn and Si, and declines in ORP and pH (Figure 3). It is possible that these high

concentrations reflect those in initial tailings dam pore waters transported with the spilled tailings, but this is unlikely for the following reasons. First, most of the tailings and interstitial water went into Quesnel Lake rather than Hazeltine Creek[25], second, we sampled in a very disturbed mixed river sediment rather than undisturbed layers of tailings and third, we sampled a year after the spill and the nature of the channel (high gradient, gravelly substrate) encouraged flushing by hyporheic exchange. Therefore, we propose that the high filtered V concentrations at 10 and 20 cm depth arose from dissolution of V-bearing phases containing these elements just below the water-sediment interface[66]. Positive trends between concentrations of V and those of Al, Fe, Cr, Mn and Si (Figure 4) suggest that one of the phases undergoing such dissolution could be the Mount Polley magnetite which incorporates these elements. The dissolution of vanadium titano-magnetite with similar concentrations of V (0.28 wt. %) has been demonstrated experimentally by Hu et al.[10], who showed that V is released from magnetite between pH 5.9 and 8.8 under dissolved O_2 ranging from 5% to 80%. Other possibilities for phases undergoing dissolution to produce these positive trends could be V-bearing clay minerals, $Al(OH)_3$ or Fe-Al-Mn-Si oxyhydroxides whose V concentrations were below detection limits of our microprobe analysis and which were small enough to pass through the 0.45 µm filter.

Vanadium concentrations in inflow waters are mostly lower than those in pore waters, and those up to 50 µg/L correlate well with Ca, Si, Fe and Al, while those up to 25 µg/L correlate with Cr and Mn (Figure 4). The released Ca and Si can be attributed to the weathering of epidote or feldspar which occur in the tailings, and that of Ca, Si, Fe and Al, to the weathering of hornblende (Supplementary Table S5), but none of these minerals were found to contain V. Ca and Si are two of the major components of titanite, and Mount Polley titanites contain trace amounts of V, Fe, Al, Cr and Mn. It is proposed that titanite weathering in the tailings piles from which the inflows emanate is responsible for these trends and modest enrichments in V. Although they did not analyze for V, Tilley and Eggleton[67] have shown that titanite can weather, likely under supergene conditions, to beidellite and anatase at neutral pH, resulting in loss of all of the Ca but retention of Ti. The reason for the

different V-trends shown by the inflows and pore waters (Figure 4) is unknown but may be related to different proportions of these minerals in the spilled tailings.

Positive saturation indices for ferrihydrite and goethite (Supplementary Table S1), the presence of Fe oxyhydroxides forming along the inflow waters and the sampled V-bearing Fe oxyhydroxide (POL-13, Supplementary Table S5, Supplementary Figure S3; Figure 5) show that some of the mobilized V is taken up by secondary Fe precipitates. Iron oxyhydroxides were observed in 2015 at the sediment-water interface in Hazeltine Creek, especially in the riparian area downstream of the second gorge where the gradient shallowed and the valley widened (near HC-9; Figure 1). These, and the declines in Fe concentrations in the Hazeltine Creek stream waters at 0 cm in the depth profiles collected (Figure 3) suggests that the high Fe pore waters at 10 cm depth were attenuated either by diffusion of aqueous V and Fe, and/or by precipitation of Fe oxyhydroxides at this interface. The V in these Fe phases is most likely to be V(V), given the dominances of this species in the stream waters, in most of the inflow waters and in the pore waters at 0 and 10 cm depth in the PHREEQC (Supplementary Table S2), and in the XANES modeling (Figure 6). The fact that filtered V concentrations for samples with pH values between 7.5 and 8.3 are higher than those with pH values greater than 8.3 (Supplementary Figure S1) is consistent with experimental studies. Dzombak and Morel[68] and Naeem et al.[8] demonstrated that V sorption to Fe oxides and hydroxides was highest between pH c. 3 and 3.5 and then decreased as pH increased from 4 to 11.6. Naeem et al. [8] attributed this decrease to competition between OH- and aqueous V anions for Fe oxide/hydroxide surface binding sites. Similarly, positive saturation indices for the Al oxyhydroxide diaspore and Al hydroxide gibbsite, and positive trends between total Al, Si and V concentrations (Supplementary Figure S2), also suggest that the formation of secondary phases such as (Al-Si-bearing) Fe oxyhydroxides, Al oxyhydroxides and hydroxides or clay minerals (see above) may attenuate aqueous V concentrations that show a decline downstream in Hazeltine Creek (Figure 2).

The association of V with Fe oxyhydroxides has been observed for streams throughout Sweden affected by natural and anthropogenic inputs of V[69], with other studies showing that

considerable transport occurs in the colloidal phase[70]. Concentrations of total V in Hazeltine Creek are higher than those of filtered V (Figure 2), and apart from three inflow water samples, total Fe, Al and Si concentrations correlate well with total V concentrations (Supplementary Figure S2), suggesting that fine particulate transport of V is significant in the catchment.

The significance of the Mount Polley tailings spill on water quality and V transport are illustrated in Figure S4 where V flux (kg yr^{-1}) and yield (kg km^{-2} yr^{-1}) are compared to unaffected regional watersheds in British Columbia and other mining-affected watercourses around the world. Transport of V in the stream is elevated compared to nearby regional streams, even when the flux data are weighted by watershed area. In addition, under high flow conditions, V yield (measured at HC-9 in 2016) was comparable to (low flow) yield values recorded in Torna Creek, Hungary, following the 2010 Ajka bauxite residue tailings spill[71]. The V transport data reported here show a larger departure from background concentrations and fluxes than those reported for Cu at Mount Polley[37]. Particulate transport of V appeared to be more dominant under high flow than low flow, suggesting physical mobilization of residual tailings could be an important transport mechanism for V during spring freshets and summer rainfall-runoff events. However, the bulk of the tailings remaining after our sampling in 2015 and 2016 were removed from the Hazeltine Creek watershed and returned to the tailings storage facility (L. Anglin, pers. comm., 2018), suggesting that the effects of such physical mobilization could be minimal in the future.

The weathering of mine tailings derived from dam failures such as Mount Polley can play a major role in V cycling in surficial environments. We have presented evidence that deposition of V-bearing tailings can lead to enhanced pore and inflow water V concentrations, especially when deposited or stored in environments where dissolution of primary (e.g. V-bearing magnetite and titanite) and secondary (V-bearing Fe and Al oxyhydroxides or clay) minerals also leads to greater V mobilization. However, these enhanced V concentrations can be naturally attenuated, and their potential ecotoxicity reduced, by formation of secondary colloidal Fe oxyhydroxides that reduce aqueous V to near background levels.

Supporting Information

Detailed water sampling and XANES methods and mineral results, pore water geochemical data, PHREEQC modelling results and plots, automated mineralogy data and V flux and yield plot. This material is available free of charge via the Internet at http://pubs.acs.org.

AUTHOR INFORMATION

Corresponding Author

E-mail: k.hudson-edwards@exeter.ac.uk; phone: +44 1326 259 489.

Notes

The authors declare no competing financial interests.

ACKNOWLEDGEMENTS

We thank Lyn Anglin, Colleen Hughes, Art Frye and Shauna Litke of Mount Polley Mining Corporation for providing site information and data, and for field support and access. We extend our special thanks to Lyn Anglin for reviewing an early version of the manuscript. We also acknowledge Phil Riby, Andy Beard, Agatha Dobosz and Patrizia Onnis for technical support. We thank Diamond Light Source for access to beamline I18 (proposal SP15046), and Konstantin Ignatyev (Station Scientist Diamond Light Source Ltd.) for support that contributed to the results presented here. We are also grateful to the three anonymous reviewers and Associate Editor Daniel Giammar whose comments significantly improved the manuscript. This research was funded by the UK Natural Environment Research Council (grant NE/M017486/1).

REFERENCES

(1) Kabata-Pendias, A. Trace Elements in Soils and Plants, 4nd ed. CRC Press, Boca Raton, FL, 2011.

(2) Imtiaz, M.; Rizwan, M. S.; Xiong, S.; Li, H.; Ashraf, M.; Shahzad, S. M.; Shahzad, M.; Rizwan, M.; Tu, S. Vanadium, recent advancements and research prospects: a review. *Environ. Int.* **2015** *80*, 79-88.

(3) Goldwaser, I.; Gefel, D.; Gershonov, E.; Fredkin, M.; Schechter, Y. Insulin-like effects of vanadium: basic and clinical implications. *J. Inorg. Biochem.* **2000** *80*, 21-25.

(4) McCrindle, C. M. E.; Mokantla, E.; N. Duncan, N. Peracute vanadium toxicity in cattlegrazing near a vanadium mine. *J. Environ. Monit.* **2001** *3*, 580-582.

(5) Yang, J.; Teng, Y.; Wu, J.; Chen, H.; Wang, G.; Song, L.; Yue, W.; Zuo, R.; Zhai, Y. Current status and associated human health risk of vanadium in soil in China. *Chemosphere* **2017** *171*, 635-643.

(6) Evangelou, A. M. Vanadium in cancer treatment. *Crit. Rev. Oncol.* **2002** *42*, 249-265.

(7) Leonard, A.; Gerber, G. Mutagenicity, carcinogenicity, and teratogenicity of vanadium, Adv. *Environ. Sci. Technol.* **1998** *31*, 143-149.

(8) Naeem, A.; Westerhoff, P.; Mustafa, S. Vanadium removal by metal (hydr)oxide adsorbents. *Water Res.* **2007** *41(7)*, 1596-1602.

(9) Huang, J. –H.; Huang, F.; Evans, L.; Glasauer, S. Vanadium: Global (bio)geochemistry. *Chem. Geol.* **2015** *417*, 8-89.

(10) Hu, X.; Yuyan, Y.; Peng, X. Release kinetics of vanadium from vanadium titano-magnetite: The effects of pH, dissolved oxygen, temperature and foreign ions. *J. Environ. Sci.* **2018** *64*, 28-305.

(11) Environment and Climate Change Canada. Canadian Environmental Protection Act, 1999. Federal Environmental Quality Guidelines. Vanadium, 2016. Available on http://www.ec.gc.ca/ese-ees/default.asp?lang=En&n=48D3A655-1, accessed 11/1/2019.

(12) Schiffer, S.; Liber, K. Estimation of vanadium water quality benchmarks for the protection of aquatic life with relevance to the Athabasca Oil Sands region using species sensitivity distributions. *Environ. Toxicol. Chem*. **2017** *36*, 3034-3044.

(13) Agency for Toxic Substances and Disease Registry (ATSDR). Toxicological profile for vanadium. U.S. Department of Health and Human Services, Public Health Service. Available on https://www.atsdr.cdc.gov/toxprofiles/tp58.pdf, 2012, accessed 2 July 2018.

(14) Jensen-Fontaine, M.; Norwood, W. P.; Brown, M.; Dixon, D. G.; Le, X. C. Uptake and speciation of vanadium in the benthic invertebrate *Hyalella Azteca. Environ. Sci. Technol.* **2014** *48*, 731-738.

(15) Mišík, M.; Burke, I. T.; Reismüller, M.; Pichler, C.; Rainer, B.; Mišíková, K.; Mayes, W. M.; Snasmueller, S. Red mud a byproduct of aluminum production contains soluble vanadium that causes genotoxic and cytotoxic effects in higher plants. *Sci. Total Environ.* **2014** *493*, 883-890.

(16) Nriagu, J.; Pirrone, N. Emission of vanadium into the atmosphere, In Nriagu, J. (Ed.) *Vanadium in the Environment, Part I: Chemistry and Biochemistry*; Wiley, New York, pp. 25-36, 1988.

(17) Shotyk, W.; Belland, R.; Duke, J.; Kempter, H.; Krachler, M.; Noernberg, T.; Pelletier, R.; Vile, M. A.; Wieder, K.; Zaccone, C.; Zhang, S., Sphagnum mosses from 21 ombrotrophic bogs in the Athabasca bituminous sands region show no significant atmospheric contamination of "heavy metals". *Environ. Sci. Technol.* **2014** *48*, 12603-12611.

(18) Yang, J.; Tang, Y.; Yang, K.; Rouff, A. A.; Elzinga, E. J.; Huang, J. H. Leaching characteristics of vanadium in mine tailings and soils near a vanadium titanomagnetite mining site. *J. Hazard. Mat.* **2014** *264*, 498-504.

(19) Cao, X.; Diao, M.; Zhang, B.; Liu, H.; Wang, S.; Yang, M. Spatial distribution of vanadium and microbial community responses in surface soil of Panzhihua mining and smelting area, China. *Chemosphere* **2017** *183*, 9-17.

(20) Watt, J. A. J.; Burke, I. T.; Edwards, R. A.; Malcom, H. M.; Mayes, W. M.; Olszewska, J. P.; Pan, G.; Graham, M. C.; Heal, K. V.; Rose, N. L.; Turner, S. D.; Spears, B. M. Vanadium: A re-emerging environmental hazard. *Environ. Sci. Technol.* **2018** *52*, 11973-11974.

(21) Burke, I. T.; Peacock, C. L.; Lockwood, D. I.; Stewart, R. J. G.; Mortimer, M. B.; Ward, P.; enforth, K.; Bruiz, W. M. Behavior of aluminum, arsenic, and vanadium during the neutralization of red mud leachate by HCl, gypsum, or seawater. *Environ. Sci. Technol.* **2013** *47*, 6527-6535.

(19) Kossoff, D.; Dubbin, W. E.; Alfredsson, M.; Edwards, S. J.; Macklin, M. G.; Hudson-Edwards, K. A. Mine tailings dams: Characteristics, failure, environmental impacts, and remediation. *Appl. Geochem.* **2014** *51*, 229-245.

(23) WISE World Information Service on Energy Uranium Project, 2018, Chronology of Major Tailings Dam Failures http://www.wise-uranium.org/mdaf.html (accessed 3 July 2018).

(24) Petticrew, E. L.; Albers, S. J.; Baldwin, S. A.; Carmack, E. C.; Dery, S. J.; Gantner, N.; Graves, K. E.; Laval, B.; Morrison, J.; Owens, P. N.; Selbie, D. T.; Vagle, S. The impact of a catastrophic mine tailings impoundment spill into one of North America's largest fjord lakes: Quesnel Lake, British Columbia, Canada. *Geophys. Res. Lett.* **2015** *42*, 3347-3355.

(25) L. Nikl, B. Wernick, J. Van Geest, C. Hughes, K. McMahen, L. Anglin, L., Mount Polley Mine embankment breach: Overview of aquatic impacts and rehabilitation. Proceedings Tailings and Mine Waste 2016, Keystone, Colorado, 2-5 October 2016, pp. 845-856.

(26) SNC-Lavalin Inc Mount Polley Mining Corporation post-event environmental impact assessment report, Appendix A: Hydrotechnical and geomorphological assessment, 621717; 2015.

(27) Independent Expert Engineering Investigation and Review Panel, Report on Mount Polley Tailings Storage Facility Breach, 2015.

(28) MPMC, Mount Polley Mining Corporation post-event environmental impact assessment report - Key findings report. Report No. Available at https://www.imperialmetals.com/assets/docs/mt-polley/2015-06-18-MPMC-KFR.pdf, 2015.

(29) Golder Associates Ltd Mount Polley Mining Corporation post-event environmental impact assessment report, Appendix F: Mount Polley Tailings Dam Failure - Surface Water Quality Impact Assessment, 1411734-036-R-Rev0-10000, 2015, pp. 1653-1984.

(30) Hudson-Edwards, K. A.; Macklin, M. G.; Jamieson, H. E.; Brewer, P. A.; Coulthard, T. J.; Howard, A. J.; Turner, J. N. The impact of tailings dam spills and clean-up on sediment and water quality in river systems: The Ríos Agrio-Guadiamar, Aznalcóllar, Spain. *Appl. Geochem*. **2003** *18*, 221-239.

(31) Bird, G.; Brewer, P. A.; Macklin, M. G.; Balteanu, D.; Serban, M.; Driga, B.; Zaharia, S. River system recovery following the Novat-Rosu tailings dam failure, Maramures County, Romania, *Appl. Geochem.* **2008** *23*, 3498-3518.

(32) Golder Associates Inc, Mount Polley rehabilitation and remediation strategy – Detailed site investigation Mount Polley tailings dam failure Mount Polley, BC. (Report No. 1411734-114-R-Rev0-11000), 2016.

(33) Golder Associates Ltd Mount Polley Mining Corporation post-event environmental impact assessment report, Appendix I: Mount Polley Tailings Dam Failure - Post-event Water Quality August 2014 through April 2015, 25 p.; 2015.

(34) Minnow Environmental Inc, Mount Polley Mining Corporation Post-even Environmental Impact Assessment Report (Appendix E: Mount Polley mine tailings dam failure: Sediment quality impact characterization), 2015.

(35) SRK Consulting (Canada) Inc, Mount Polley Mine Tailings Dam Failure: Update on Geochemical Characterization of Spilled Tailings (Vancouver, Canada), 2015.

(36) SRK Consulting (Canada) Inc Mount Polley Mining Corporation post-event environmental impact assessment report. Appendix C: Mount Polley Tailings Dam Failure - Geochemical characterisation of spilled tailings, 1CI008.003, 2015.

(37) Byrne, P.; Hudson-Edwards, K. A.; Bird, G.; Macklin, M. G.; Brewer, P. A.; Williams, R D.; Jamieson, H. E. Water quality impacts and river system recovery following the 2014 Mount Polley mine tailings dam spill, British Columbia, Canada. *Appl. Geochem*. **2018** *91*, 64-74.

(38) McMillan, W. J. Porphyry deposits of the Canadian cordillera. *Geosci. Can.* **1996** *23*, 125-134.

(39) Minnow Environmental Inc., Mount Polley Mine Aquatic Environmental Characterization - 2007, 2009.

(40) Ball, J. W.; Nordstrom, D. K. User's manual for WATEQ4F, with revised thermodynamic database and test cases for calculating speciation of major, trace, and redox elements in natural waters. U.S. Geol. Surv. Open-File Rep. 1991, 91-183, 189.

(41) Parkhurst, D. L.; Appelo, C. A. J. Description of input and examples for PHREEQC version 3: a computer program for speciation, batch-reaction, one-dimensional transport, and inverse geochemical calculations. US Geological Survey Techniques and Methods, book 6, chap. A43, 497 p.; 2013.

(42) Ravel, B. Newville, M. ATHENA, ARTEMIS, HEPHAESTUS: data analysis for X-ray absorption spectroscopy using IFEFFIT. *J. Synchrotron Radiat.* **2005** *12*, 537-541.

(43) Chaurand, P.; Rose, J.; Briois, V.; Salome, M.; Proux, O.; Nassif, V.; Olivi, L.; Susini, J.; Hazemann, J. –L.; Bottero, J. –Y. New methodological approach for the vanadium K-edge X-ray absorption near-edge structure interpretation: Application to the speciation of vanadium in oxide phases from steel slag. *J. Phys. Chem. B* **2007** *111*, 5101-5110.

(44) Burke, I. T.; Mayes, W. M.; Peacock, C. L.; Brown, A. P.; Jarvis, A. P.; Bruiz, K. Speciation of arsenic, chromium, and vanadium in red mud samples from the Ajka spill site, Hungary, *Environ. Sci. Technol*. **2012** *46*, 3085-3092.

(45) Shiller, A. M.; Boyle, E. A. Dissolved vanadium in rivers and estuaries. *Earth Planet. Sci. Lett*. **1987** *86*, 214-224.

(46) Wright, M. T.; Stollenwerk, K. G.; Belitz, K. Assessing the solubility controls on vanadium in groundwater, northeastern San Joaquin Valley, CA. *Appl. Geochem.* **2014** *48*, 41-52.

(47) Wehrli, B.; Stumm, W. Vanadyl in natural waters: Adsorption and hydrolysis promote oxygenation. *Geochim. Cosmochim. Acta* **1989** *53*, 69-77.

(49) Lu, X.Q.; Johnson, W.D.; Hook, J. Reaction of vanadate with aquatic humic substances: an ESR and V-51 NMR study. *Environ. Sci. Technol*. *32*, 2257-22263.

(50) Levshina, S. An assessment of metal-humus complexes in river waters of the Upper Amur basin, Russia. *Environ. Monit. Assess*. **2018** *190*, 18.

(50) Wong, H. K. T., Gauthier, A.; Nriagu, J. O. Dispersion and toxicity of metals from abandoned gold mine tailings at Goldenville, Nova Scotia, Canada. *Sci. Total Environ*. **1999** *228*, 35-47.

(51) Gleisner, M.; Herbert, R. B. Sulfide mineral oxidation in freshly processed tailings: batch experiments. *J. Geochem. Explor.* **2002** *76*, 139-153.

(52) Kennedy, C. B.; Day, S. J.; Anglin, C. D. Geochemistry of tailings from the Mount Polley Mine, British Columbia, Proceedings Tailings and Mine Waste 2016, Keystone, Colorado, USA, 2-5 October 2016, pp. 857-868.

(53) Celis, A. Titanite as an indicator mineral for alkalic porphyry Cu-Au deposits in south-central British Columbia, UBC Library, doi 10.14288/1.0166663, 2015.

(54) Peacock, C. L.; Sherman, D. M. Vanadium(V) adsorpton onto goethite (α-FeOOH) at pH 1.5 to 12: a surface complexation model based on ab initio molecular geometries and EXAFS spectroscopy. *Geochim. Cosmochim. Acta* **2004** *68*, 1723-1733.

(55) Chaurand, P.; Rose, J.; Briois, V.; Salome, M.; Proux, O.; Nassif, V.; Olivi, L.; Susini, J.; Hazemann, J. -L.; Bottero, J. -Y. New methodological approach for the vanadium K-edge X-ray absorption near-edge structure interpretation: Application to the speciation of vanadium in oxide phases from steel slag. *J. Phys. Chem. B* **2007** *111*, 5101 − 5110.

(56) Hobson A. J.; Stewart D. I.; Bray A. W.; Mortimer R. J. G.; Mayes W. M.; Riley A. L.; Rogerson M.; Burke I. T. Behaviour and fate of vanadium during the aerobic neutralisation of hyperalkaline slag leachate. *Sci. Total Environ.* **2018** *643*, 1191-1199.

(57) Toplis, M. J.; Corgne, A. An experimental study of element partitioning between magnetite, clinopyroxene and iron-bearing silicate liquids with particular emphasis on vanadium. *Contrib. Mineral. Petrol.* **2002** *144*, 22-37.

(58) Balan, E.; de Villiers, J. P. R.; Eeckhout, S. G.; Glatzel, P.; Toplis, M. J.; Fritsch, E.; Allard, T.; Galoisy, L.; Calas, G. The oxidation state of vanadium in titanomagnetite from layered basic intrusions. *Am. Mineral.* **2006** *91*, 953-956.

(59) Canil, D.; Grondahl, C.; Lacourse, T.; Pisiak, L. K. Trace elements in magnetite from porphyry Cu-Mo-Au deposits in British Columbia, Canada. *Ore Geol. Rev.* **2016** *72*, 1116-1128.

(60) Pan, Y.; Fleet, M. E. Vanadium-rich minerals of the pumpellyite group from the Hemlo gold deposit, Ontario. *Can. Mineral.* **1992** *30*, 153-162.

(61) Shannon, R. D. Revised effective ionic radii and systematic studies of interatomic distances in halides and chalcogenides. *Acta Crystallogr.* **1976** *A32*, 751-767.

(62) Wehrli, B.; Stumm, W. Vanadyl in natural waters - Adsorption and hydrolysis promote oxygenation. *Geochim. Cosmochim. Acta* **1989** *53*, 69-7.

(63) U. Schwertmann, U.; Pfab, G. Structural vanadium in synthetic goethite. *Geochim. Cosmochim. Acta* **1994** *58*, 4349-4352.

(64) Larsson, M. A.; Persson, I.; Sjöstedt, C.; Gustafsson, J. P. Vanadate complexation to ferrihydrite: X-ray absorption spectroscopy and CD-MUSIC modelling. *Environ. Chem.* **2016** *14*, 141-150.

(65) Kaur, N.; Singh, B.; Kennedy, B. J.; Gräfe, M. The preparation and characterization of vanadium-substituted goethite: The importance of temperature. *Geochim. Cosmochim. Acta* **2009** *73*, 582-593.

(66) Surridge, B. W. J.; Heathwait, A. L.; Baird, A. J. The release of phosphorus to porewater and surface water from river riparian sediments. *J. Environ. Qual*. **2007** *36*, 1534-1544.

(67) Tilley, D. B.; Eggleton, R. A. Titanite low-temperature alteration and Ti mobility. *Clays Clay Miner.* **2005** *53*, 100-107.

(68) Dzombak, D. A.; Morel, F. M. M. Surface Complexation Modelling: Hydrous Ferric Oxide. Wiley-Interscience, New York, 1990.

(69) Wällstedt, T.; Björkvald, L.; Gustafsson, J. P. Increasing concentrations of arsenic and vanadium in (southern) Swedish streams. *Appl. Geochem.* **2010** *25*, 1162-1175.

(70) Dahlqvist, R.; Andersson, K.; Ingri, J.; Larsson, T.; Stolpe, B.; Turner, D. Temporal variations of colloidal carrier phases and associated trace elements in a boreal river. *Geochim. Cosmochim. Acta* **2007** *71*, 5339-5354.

(71) Mayes, W. M.; Jarvis, A. P.; Burke, I. T.; Walton, M.; Feigl, V.; Klebercz, O.; Gruiz, K. Dispersal and attenuation of trace contaminants downstream of the Ajka bauxite residue (red mud) depository failure, Hungary. *Environ. Sci. Technol*. **2011** *45*, 5147-5155.

(72) Hobson, A. J. Stewart, D. I.; Bray, A. W.; Mortimer, R. J. G.; Mayes, W. M.; Rogerson, M.; Burke, I. T. Mechanism of vanadium leaching during surface weathering of basic oxygen furnace steel slag blocks: A microfocus X-ray absorption spectroscopy and electron microscopy study. *Environ. Sci. Technol.* **2017** *51*, 7823-7830.

(73) Bronkema, J. L.; Bell, A. T. Mechanistic studies of methanol oxidation to formaldehyde on isolated vanadate sites supported on MCM-48. *J. Phys. Chem*. C **2007** *111*, 420-430.

(74) Wong, J.; Lytle, F. W.; Messmer, R. P.; Maylotte, D. H. K-edge absorption-spectra of selected vanadium compounds. *Phys. Rev. B* **1984** *30*, 5596-5610.

Figure 1. Location of study area showing Hazeltine Creek stream (HC-), inflow sample, pore water (PW-) and tailings, sediment and Fe oxyhydroxide (POL-) sample sites for materials collected in 2014 and 2015. Labels shown are for those samples discussed in this manuscript; sample locations for the remaining stream, inflow and pore water samples are shown in Byrne et al.[37].

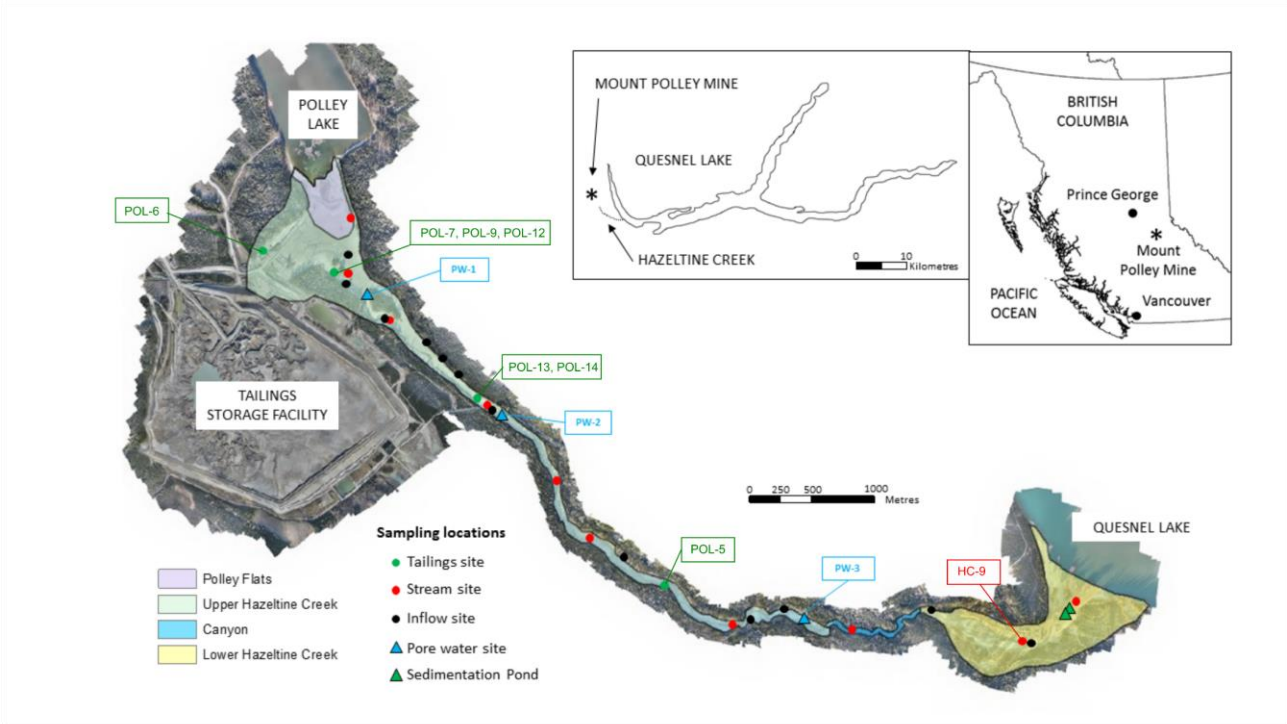

Figure 2. Spatial profile of Hazeltine Creek stream and inflow filtered (V-F) and unfiltered (V-T) V concentrations. Samples were collected in August 2015. Pre-tailings dam spill median V concentration of 1 µg/L[29] is shown for reference.

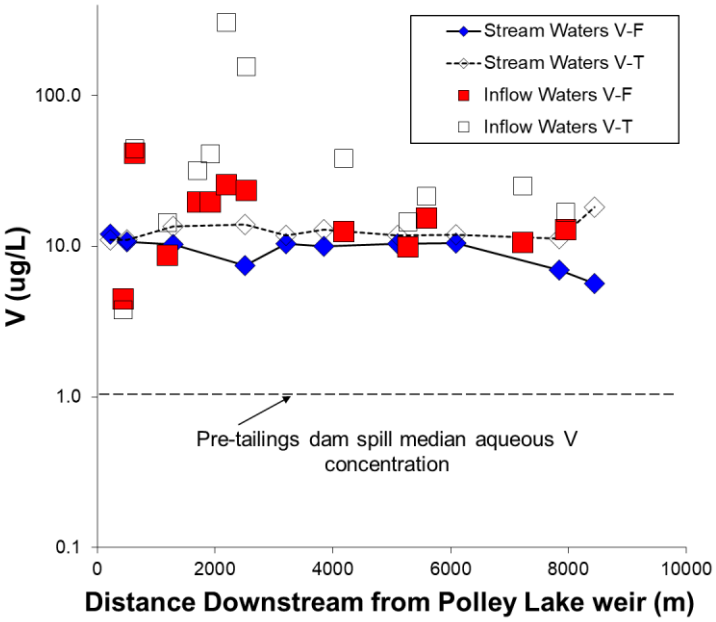

Figure 3. Geochemical profiles for pore water profiles PW-1, PW-2 and PW-3.

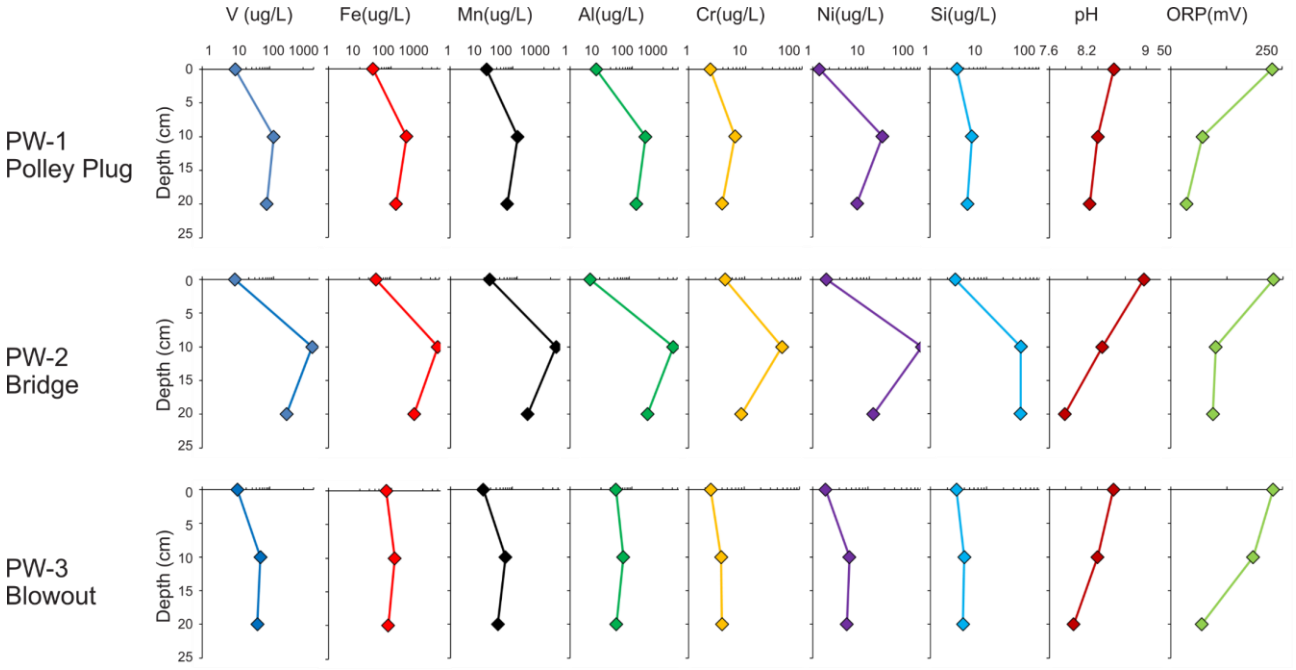

Figure 4. X-Y plots showing relationship between filtered V (µg L^{-1}) and other filtered element concentrations in stream, inflow and pore waters. Stream water sample concentrations are mostly < 10 µg/L so are masked by the inflow and pore waters. Trends shown for the inflow waters (red squares) and for most of the pore water data (green circles).

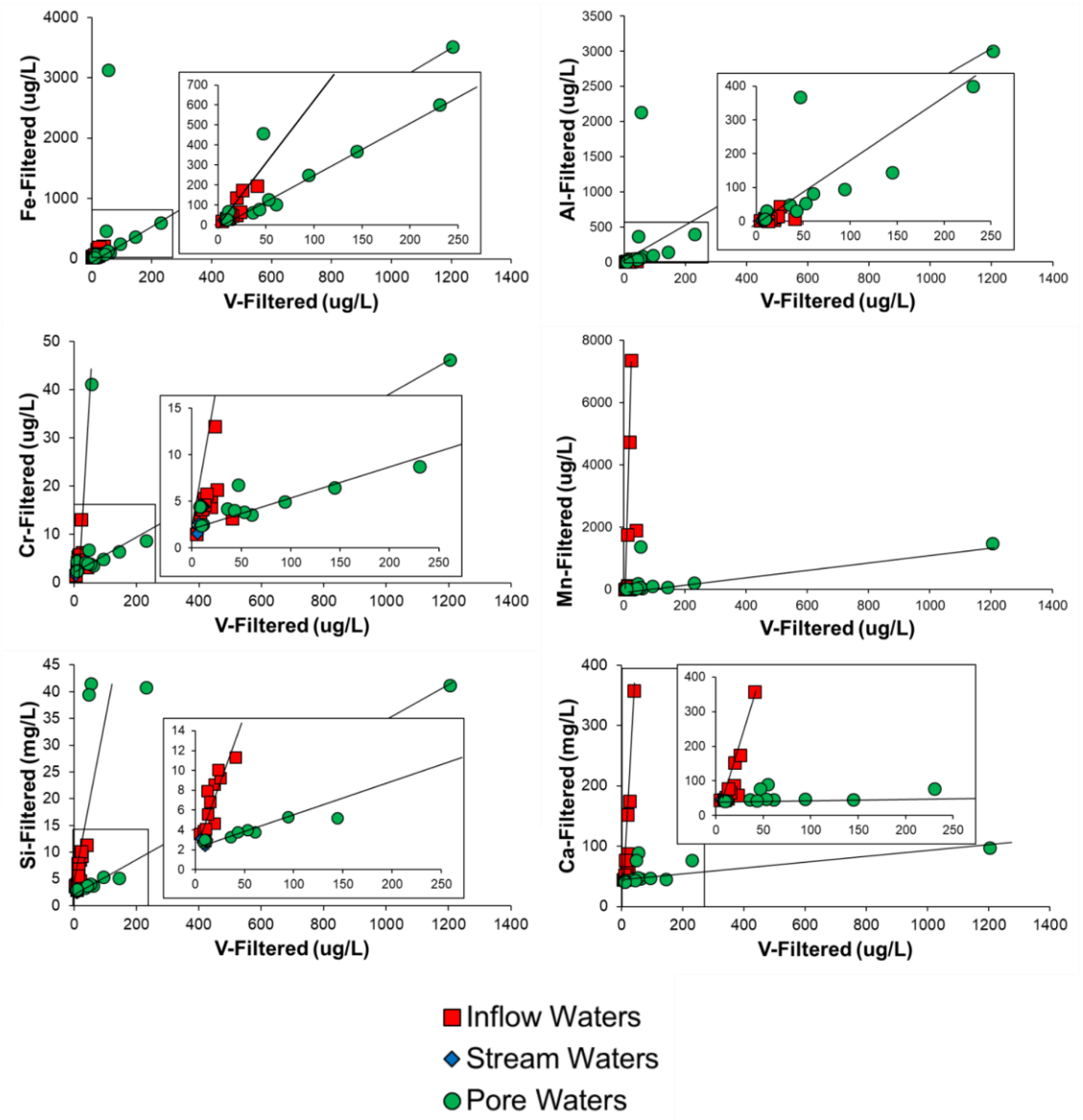

Figure 5. Electron microprobe X-ray maps showing V-bearing titanite and magnetite in Mount Polley tailings (POL-5), and V-bearing Fe oxide in the Fe oxyhydroxide (Fe oxyhyd) (POL-13).

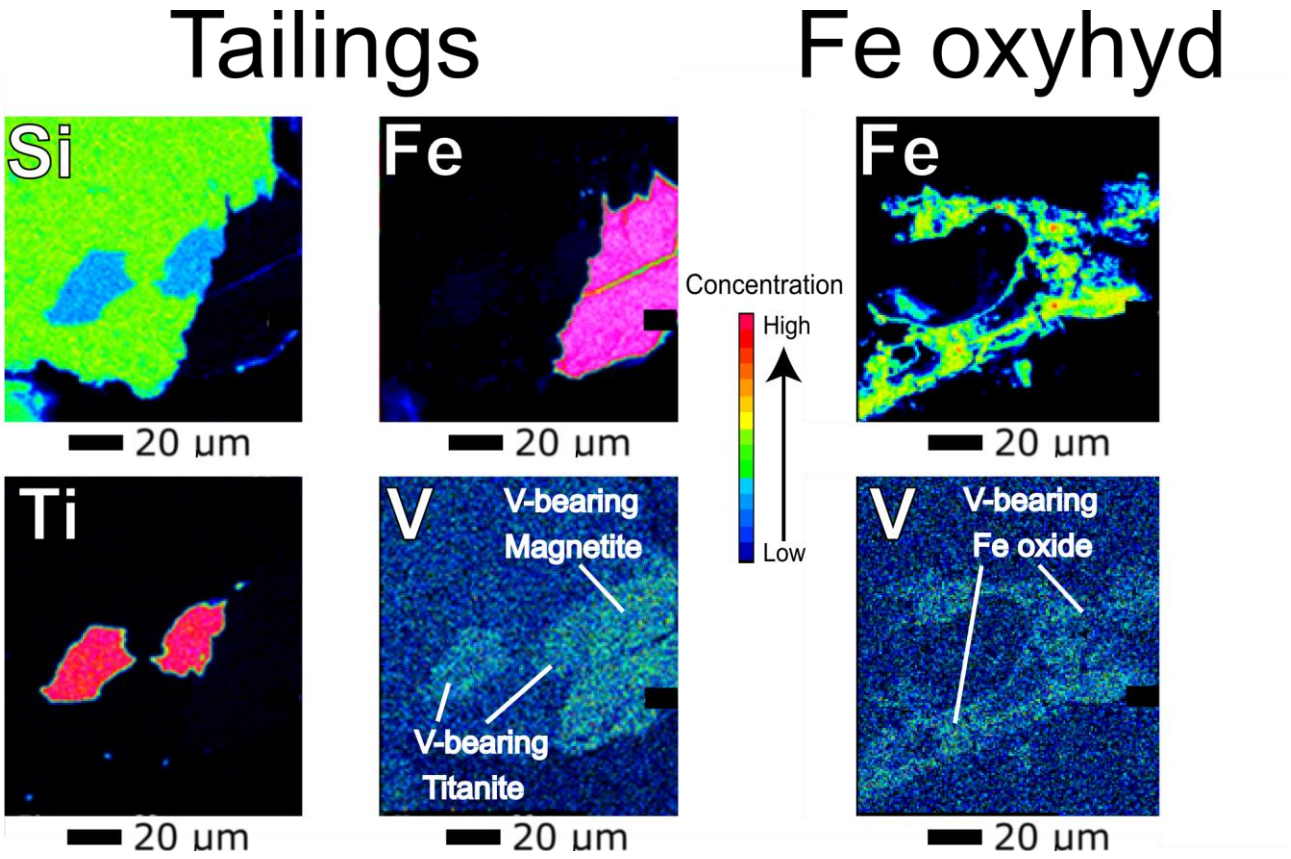

Figure 6. (a) K-edge XANES spectra collected from Mount Polly mineral samples and selected V-containing standards. (b) Plot of pre-edge intensity vs. pre-edge peak energy derived from V K-edge XANES spectra. V standard data from Hobson et al.[72], Burke et al.[21,44], Charaund et al.[43], Bronkema and Bell[73] and Wong et al.[74]. (T_d), (P_y) and (O_h) refer to tetrahedral, square pyramidal and octahedral co-ordination, respectively.

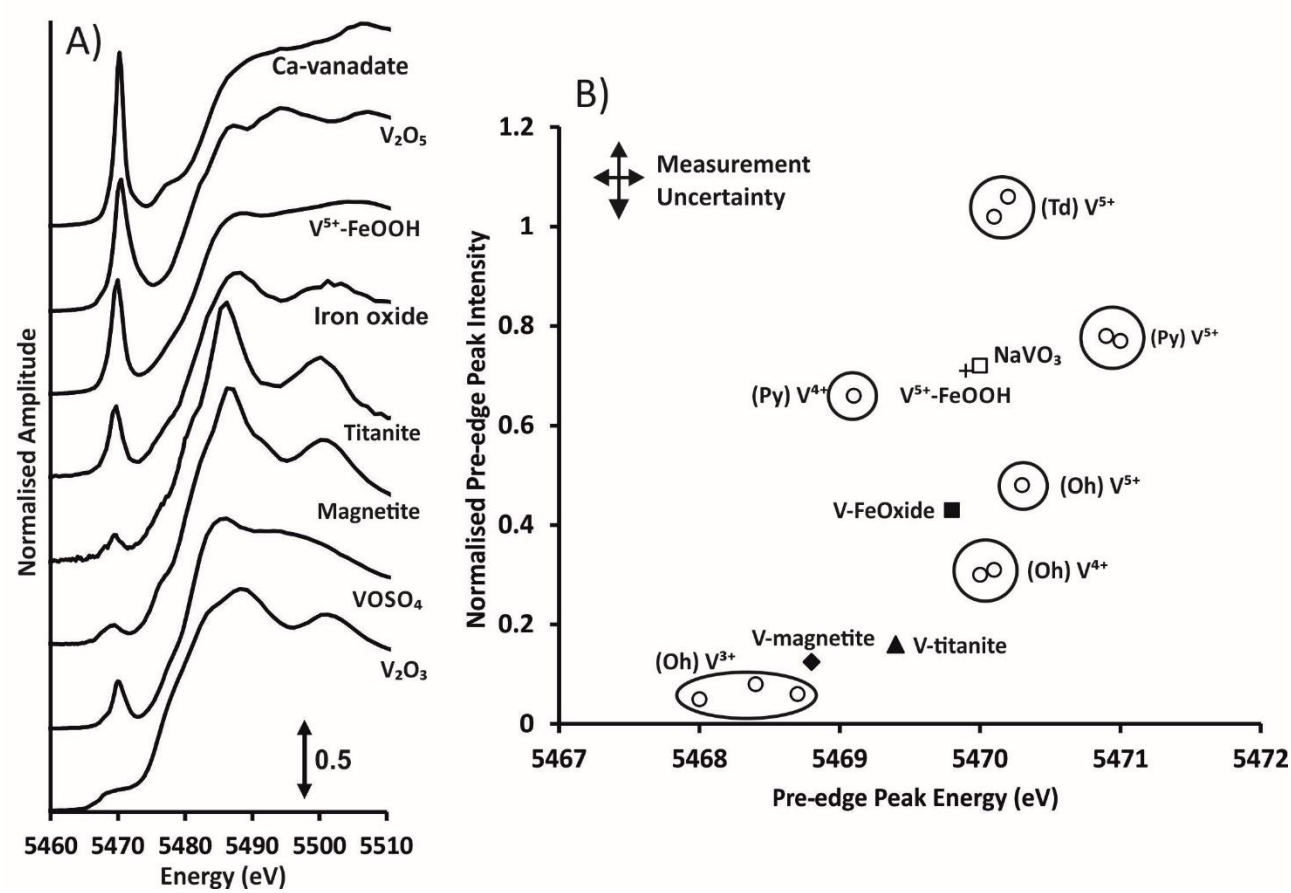

Origin and fate of Vanadium in the Hazeltine Creek Catchment following the 2014 Mount Polley mine tailings spill, British Columbia, Canada

Karen A. Hudson-Edwards[1], Patrick Byrne[2], Graham Bird[3], Paul A. Brewer[4], Ian T. Burke[5], Heather E. Jamieson[6], Mark G. Macklin[7], Richard D. Williams[8]*

[1] Environment & Sustainability Institute and Camborne School of Mines, University of Exeter, Penryn Cornwall TR10 9FE, UK. *Corresponding author. Email k.hudson-edwards@exeter.ac.uk; Tel: +44-(0)1326-259-489.

[2] School of Natural Sciences and Psychology, Liverpool John Moores University, Liverpool, L3 3AF, UK. Email p.a.byrne@ljmu.ac.uk

[3] School of Environment, Natural Resources and Geography, Bangor University, Bangor, Gwynedd, LL57 2UW, UK. g.bird@bangor.ac.uk

[4] Department of Geography and Earth Sciences, Aberystwyth University, Penglais, Aberystwyth, Ceredigion WY23 3FL, UK. pqb@aber.ac.uk

[5] School of Earth and Environment, University of Leeds, Leeds LS2 9JT, UK. i.t.burke@leeds.ac.uk

[6] Department of Geological Sciences and Geological Engineering, Queen's University, Kingston, Ontario K7L 3N6, Canada. jamieson@queensu.ca

[7] Lincoln Centre for Water and Planetary Health, School of Geography, College of Science, University of Lincoln, Brayford Pool, Lincoln, Lincolnshire LN6 7TS, UK. mmacklin@lincoln.ac.uk

[8] School of Geographical and Earth Sciences, University of Glasgow, Glasgow G12 8QQ, UK. Richard.Williams@glasgow.ac.uk

Submitted to: *Environmental Science & Technology*

Accepted: 4 March 2019

Keywords: Vanadium; Mount Polley; tailings; magnetite; titanite; XANES

Supporting Information

Supplementary Information: Methodology

Field data collection

As described in Byrne et al.[1], a synoptic survey of water quality under low flow conditions was conducted in Hazeltine Creek on August 2nd 2015. High flow samples were collected at selected locations in 2016. The samples were collected when active creek reconstruction and remediation activities were being carried out. At each water sampling location, physico-chemical parameters (pH, specific conductivity and Eh) were measured using an AQUAREAD AP-5000 multi-parameter probe following appropriate calibration protocols. Alkalinity was estimated as bicarbonate by ion sum calculation. Three stream water samples were collected at each sample location for determination of major ion and trace element concentrations. Samples for total cation and trace metal analysis were preserved with concentrated HNO_3. Samples for filtered cation and trace metal analysis were filtered through a 0.45 μm cellulose nitrate filter before acidification, whereas those for anion analysis were filtered only. Physico-chemical measurements for pore water samples were made using the AQUAREAD probe and a flow-through cell. Treatment of pore water samples for ion and trace metal analyses followed the same procedure as above for stream samples.

Water quality analyses

Analytical accuracy for the cation (ICP-OES – Thermo Scientific iCAP 6500 Duo) and trace metal (ICP-MS – Thermo X-series 2) analyses was assessed using the certified reference material SLRS-6 (National Research Council of Canada). Analytical accuracy for the anion (DIONEX ICS-2500) analyses was assessed using the certified reference material BATTLE-02 (National Water Research Institute, Environment Canada). Instrument and analytical precision for the ICP-OES, ICP-MS and Dionex IC, monitored using blind duplicates, was found to be ±5%.

Preparation of V(V)-FeOOH XANES standard

The V(V)-FeOOH standard was prepared by adding 20 mL 100 ppm $NaVO_3$ dropwise over 20 min to 0.2 g goethite suspended in 2 L Milli-Q DIW to achieve a sorbed V concentration of ~1 wt %. Solution pH was maintained at pH 8 by adding 0.1 M HCl or 0.1 M NaOH as required. Once all $NaVO_3$ had been added the suspension was left overnight prior to vacuum filtering at 0.2 μm. The residue was dried in an oven at 40 °C for 24 h.

Supplementary Information: Results

Supplementary Figure S1. V-filtered (µg/L) versus pH for Hazeltine Creek stream, inflow and pore waters. Grey bar shows the boundaries for the transition from HVO_4^{2-} (> pH c. 8.1-8.3) to $H_2VO_4^-$ (<pH c. 8.1-8.3)[2,3].

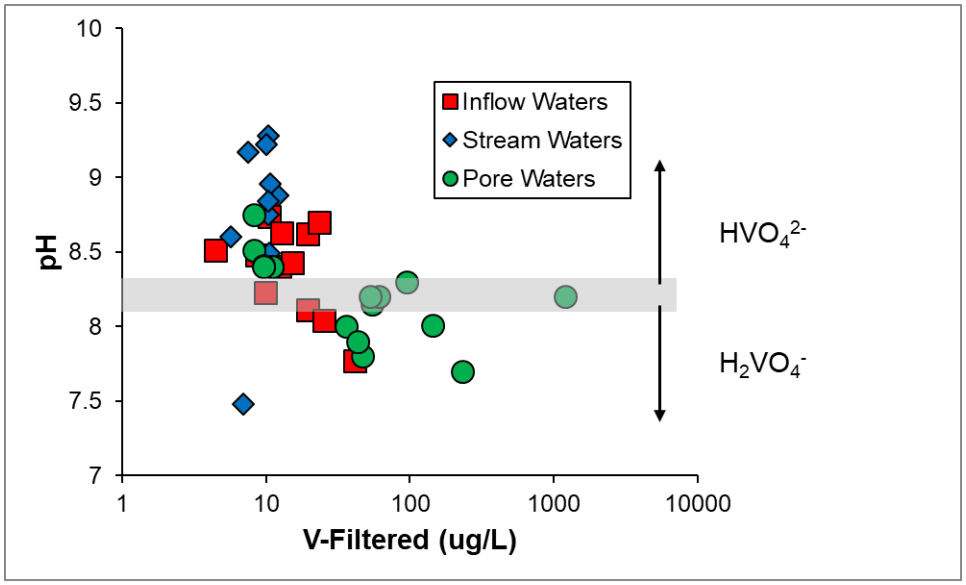

Supplementary Figure S2. V-total (µg/L) versus Fe-total (µg/L), Al-total (µg/L) and Si-total (µg/L) for Hazeltine Creek stream and inflow waters.

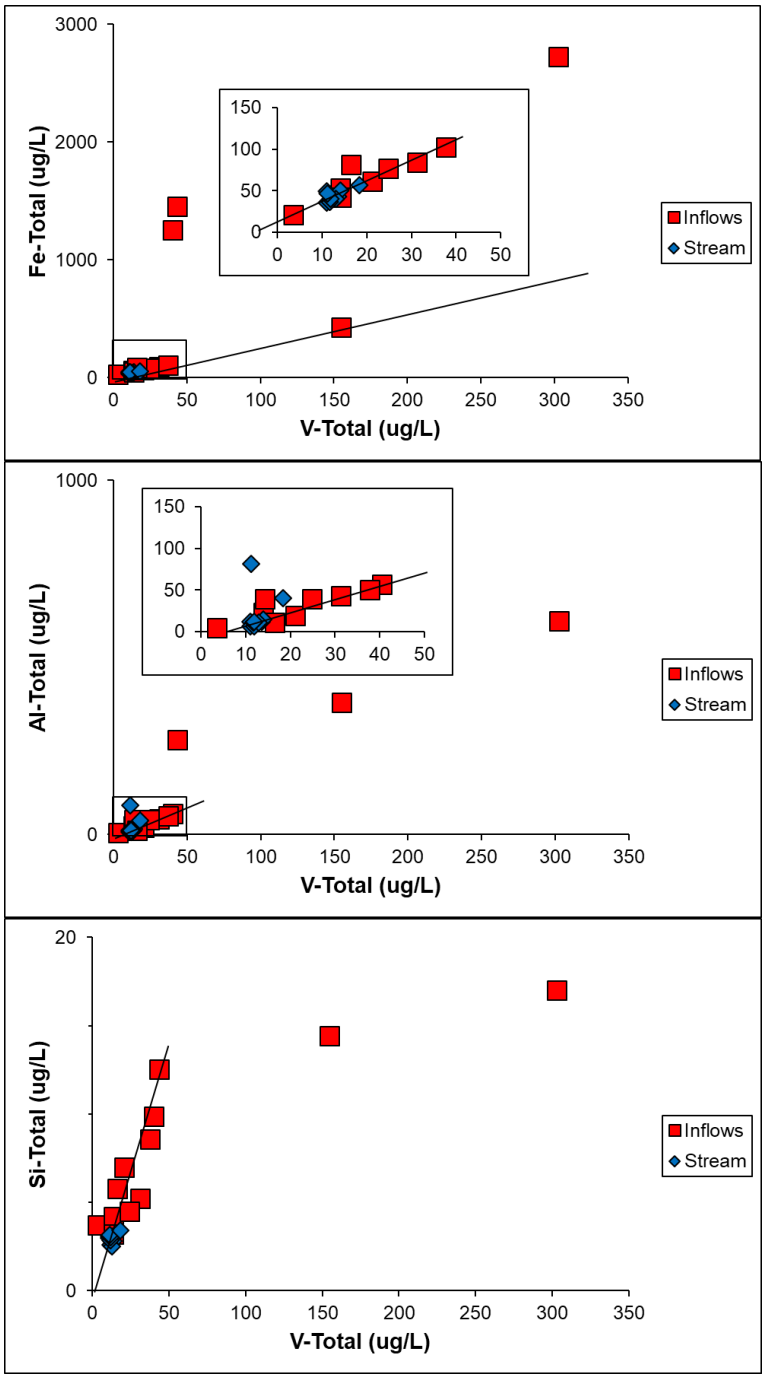

Supplementary Figure S3. Photograph taken in August 2015 near site of sample S-1 (Figure 1), showing orange-yellow Fe oxyhydroxides forming in water seeping from beneath deposited tailings. This is an example of a low-flow seep which were present in 2015 though not volumetrically significant in the Hazeltine Creek catchment.

Supplementary Figure S4. V flux and yield for Hazeltine Creek (HC-9 in 2016[1]), regional streams (background) and worldwide streams (mining-affected). Note the logarithmic axes. Hazeltine Creek: HF=high flow; LF=low flow; T=total load; F=filtered load. Regional streams: WC = Winkley Creek; CubC = Cub Creek; CedarC = Cedar Creek; EC = Edney Creek; LC = Lion Creek (USA)[6]; Tor = Torna Creek (Hungary)[7].

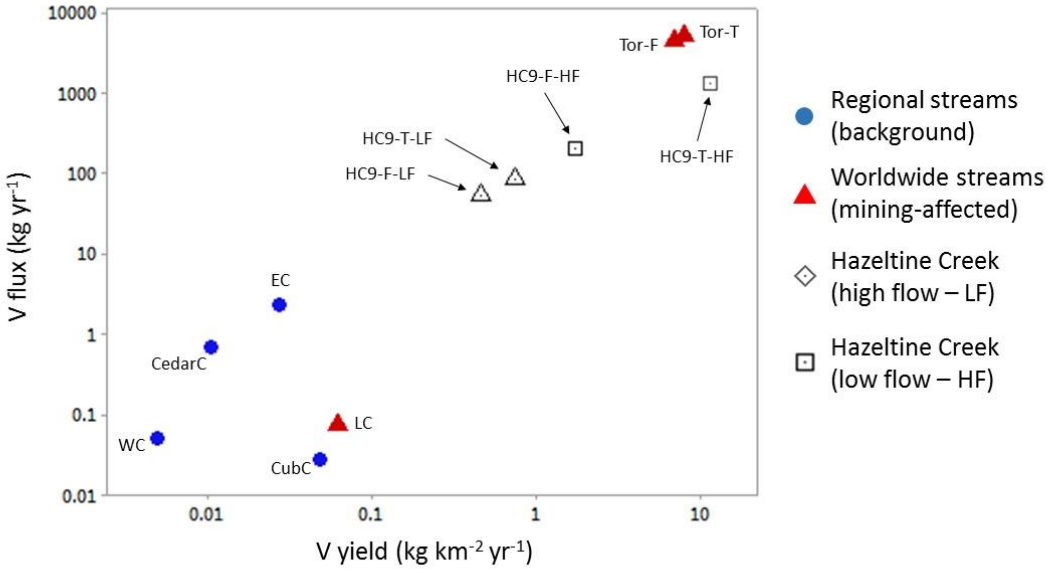

Supplementary Table S1. Mineral saturation indexes based on Hazeltine Creek stream and pore water compositions given in Byrne et al.[1] (Table S1). Results based on PHREEQC modelling[4]. Major phases calculated using data from the minteq.dat.v4 database.

Phase	Species	Hazeltine Creek	Inflows	Pore waters
$Al(OH)_3am$	$Al(OH)_3am$	-4.53 to -2.74	-4.33 to -1.87	-2.96 to -1.16
$Ca_2V_2O_7$	$Ca_2V_2O_7$	-8.95 to -6.20	-18.01 to -5.59	-17.57 to -2.72
$Ca_3(VO_4)_2$	$Ca_3(VO_4)_2$	-18.55 to -12.55	-26.89 to -13.00	-26.62 to -11.30
Ca-vanadate	$Ca_{0.5}VO_3$	-9.58 to -8.38	-19.23 to -7.93	-18.31 to -3.93
Fe-vanadate	$Fe_{0.5}VO_3$	-9.80 to -4.70	-13.09 to -4.93	-12.07 to -1.13
Mg-vanadate	$Mg_{0.5}VO_3$	-15.81 to -14.64	-25.45 to -13.83	-24.60 to -9.98
$Mg_2V_2O_7$	$Mg_2V_2O_7$	-18.74 to -16.26	-28.01 to -15.27	-27.76 to -12.42
Mn-vanadate	$Mn_{0.5}VO_3$	-13.22 to -11.41	-21.27 to -8.65	-20.47 to -5.18
Na_3VO_4	Na_3VO_4	-31.84 to -28.92	-35.72 to -27.76	-35.99 to -28.63
$Na_4V_2O_7$	$Na_4V_2O_7$	-36.00 to -33.34	-44.60 to -30.81	-44.74 to -30.30
Na-vanadate	$NaVO_3$	-7.59 to -6.96	-12.13 to -6.22	-11.93 to -4.85
$V(OH)_3$	$V(OH)_3$	-16.38 to -11.66	-13.80 to -10.60	-13.88 to -10.16
V_2O_5	V_2O_5	-17.70 to -13.80	-24.91 to -14.38	-23.74 to -9.83
V_3O_5	V_3O_5	-34.08 to -21.31	-27.35 to -20.01	-27.43 to -16.99
V_4O_7	V_4O_7	-42.62 to -26.83	-34.36 to -25.39	-34.31 to -20.86
V_6O_{13}	V_6O_{13}	-39.06 to -22.58	-44.27 to -22.66	-41.82 to -11.99
VCl_2	VCl_2	-69.32 to -57.42	-62.86 to -51.99	-62.23 to -52.48
VMetal	VMetal	-87.97 to -76.34	-82.69 to -69.81	-83.02 to -69.30
VO	VO	-35.34 to -28.16	-31.87 to -25.46	-32.03 to -25.65
$VO(OH)_2$	$VO(OH)_2$	-8.38 to -5.33	-7.44 to -5.05	-7.45 to -3.47
VO_2Cl	VO_2Cl	-28.16 to -22.95	-28.16 to -22.57	-27.54 to -18.94
$VOSO_4$	$VOSO_4$	-29.94 to -22.19	-26.82 to -23.37	-25.17 to -18.04
Calcite	$CaCO_3$	-0.14 to 1.40	0.58 to 1.54	0.27 to 0.75
Diaspore	AlOOH	-0.59 to 1.18	-0.39 to 2.07	0.99 to 3.95
Gibbsite	$Al(OH)_3$	6.48 to 8.12	-1.80 to 0.67	-0.41 to 2.56

Supplementary Table S2. Distribution of V^{3+} and V^{5+} dissolved species (in %) for the Hazeltine Creek stream, inflow and pore waters, as obtained from PHREEQC equilibrium calculations. Calculations were not carried out for PW-1_0 or PW-1_20 because no Cl^- or SO_4^{2-} data were available for these samples.

Sample	**V^{3-}**	**V^{5+}**		**V^{3-}**	**V^{5+}**		**V^{3-}**	**V^{5+}**
Stream waters			*Inflow waters*			*Pore waters*		
HC1	0	100	S1	0	100	PW-1_10	51	49
HC2	0	100	S2	100	0	PW-2_0	1	99
HC3	0	100	S3	0	100	PW-2_10	0	100
HC4	0	100	S4	0	100	PW-2_20	75	25
HC5	0	100	S5	6	94	PW-3_0	2	98
HC6	0	100	S6	77	23	PW-3_10	24	76
HC7	0	100	S7	0	100	PW-3_20	91	9
HC8	1	99	S8	100	0			
HC9	65	35	S9	11	89			
HC10	0	100	S10	7	93			
			S11	11	89			
			S12	1	99			

Supplementary Table S3. Distribution of HVO_4^{2-} and $H_2VO_4^-$ dissolved species (in %) for the Hazeltine Creek stream, inflow and pore waters, as obtained from PHREEQC equilibrium calculations. Calculations were not carried out for PW-1_0 or PW-1_20 because no Cl^- or SO_4^{2-} data were available for these samples.

Sample	**HVO_4^{2-}**	**$H_2VO_4^-$**		**HVO_4^{2-}**	**$H_2VO_4^-$**		**HVO_4^{2-}**	**$H_2VO_4^-$**
Stream waters			*Inflow waters*			*Pore waters*		
HC2	75	25	S2	23	77	PW-1_10	30	70
HC3	64	36	S3	51	49	PW-2_0	46	54
HC4	83	17	S4	61	39	PW-2_10	34	66
HC5	86	14	S5	55	45	PW-2_20	21	79
HC6	84	16	S6	31	69	PW-3_0	45	55
HC7	69	31	S7	63	37	PW-3_10	34	66
HC8	50	50	S8	49	51	PW-3_20	29	71
HC9	9	91	S9	36	64			
HC10	57	43	S10	49	51			
			S11	36	64			
			S12	60	40			

Supplementary Table S4. Tailings and Fe oxyhydroxide sample descriptions and V concentrations. Samples POL-5 and POL-6 were donated by Mount Polley Mining Corporation, and further details are given in SNC-Lavalin Inc[5]. The remaining samples were collected by the authors in August 2015.

Sample	Sample Date	Sample Description	V (mg/kg)
POL-5	15/09/2014	Tailings (ST 09-02-01-140915)	170
POL-6	12/09/2014	Tailings (WT 17-08-02-140912)	231
POL-7	12/07/2016	Tailings (magnetite sand) deposit c. 1.5 m thick	205
POL-9	12/07/2016	Tailings (magnetite sand) deposit c. 1 m thick	85
POL-12	12/07/2016	Magnetite sand scraped from seep draining tailings	51
POL-13	12/07/2016	Ochre deposit scraped from seep draining re-profiled stream bank	185
POL-14	12/07/2016	Tailings (magnetite sand) deposit between rock armour on stream bank	124

Supplementary Table S5. Automated mineralogical analysis of Hazeltine Creek tailings, sediment and ochre samples. Minerals with area % abundances < 0.03% for all samples are not included.

	POL5	POL6	POL7	POL9	POL12	POL13	POL14
Mineral	Area%	Area%	Area%	Area%	Area%	Area%	Area%
Fe Oxides	3.05	2.38	2.40	1.16	0.58	4.70	1.62
Cu-bearing Fe oxide	2.32	1.91	0.63	0.51	0.67	4.32	0.64
Titanite	0.67	0.46	1.69	0.73	0.46	1.44	1.28
Epidote	4.67	4.83	4.92	3.52	0.81	3.70	3.97
Hornblende/Augite	5.07	4.72	4.14	3.88	7.21	10.70	4.63
Enstatite	0.00	0.00	0.00	0.00	0.19	0.00	0.00
Chlorite	1.39	1.33	1.47	1.77	0.84	2.04	1.16
Orthoclase	38.13	39.07	39.50	41.14	7.01	20.31	28.11
Albite	32.26	32.71	32.98	34.68	16.24	20.18	22.28
Plagioclase	2.27	2.35	1.60	2.46	3.05	2.43	1.73
Quartz	1.56	1.30	1.85	2.37	50.36	20.23	27.18
Apatite	0.37	0.38	0.34	0.26	0.12	0.16	0.26
Muscovite	3.21	3.38	3.65	3.77	10.11	3.76	2.97
Ilmenite	0.05	0.04	0.03	0.02	0.15	0.05	0.02
Ti-Fe-Ca-Si phase	0.01	0.00	0.04	0.02	0.00	0.04	0.03
Ilmenorutile	0.06	0.06	0.06	0.02	0.10	0.13	0.04
Rutile	0.01	0.01	0.01	0.00	0.03	0.01	0.01
Fe Ti Silicate	0.01	0.01	0.01	0.00	0.01	0.06	0.00
Ti-Muscovite	0.30	0.34	0.40	0.27	0.41	0.38	0.26
Vermiculite	1.55	1.61	1.92	1.02	0.14	1.65	1.34
Calcite	1.67	1.83	1.94	2.04	0.48	1.55	1.57
Ankerite	0.10	0.07	0.05	0.03	0.09	0.57	0.04
Dolomite	0.00	0.00	0.00	0.00	0.00	0.01	0.05
Chalcopyrite	1.05	1.09	0.12	0.12	0.00	0.03	0.04
Pyrite	0.10	0.08	0.08	0.04	0.00	0.02	0.04

Supplementary Table S6. V K-edge XANES data measured for minerals present in Mount Polly samples.

Sample	**Pre-edge Peak Energy (±0.3 eV)**	**Normalised pre-edge peak height (±0.10)**	**Main adsorption edge $E_{1/2}$ (±0.3 eV)**
Magnetite	5468.8	0.13	5478.3
Titanite	5469.4	0.16	5478.6
Iron oxide	5469.8	0.43	5479.7

References

(1) Byrne, P.; Hudson-Edwards, K. A.; Bird, G.; Macklin, M. G.; Brewer, P. A.; Williams, R D.; Jamieson, H. E. Water quality impacts and river system recovery following the 2014 Mount Polley mine tailings dam spill, British Columbia, Canada. *Appl. Geochem*. **2018** *91*, 64-74.

(2) Wright, M. T.; Stollenwerk, K. G.; Belitz, B. K. Assessing the solubility controls on vanadium in groundwater, northeastern San Joaqin Valley, CA. *Appl. Geochem*. **2014** *48*, 41-52.

(3) Huang, J. –H.; Huang, F.; Evans, L.; Glasauer, S. Vanadium: Global (bio)geochemistry. *Chem. Geol.* 417 **2015** *417*, 8-89.

(4) Parkhurst, D. L.; Appelo, C. A. J. Description of input and examples for PHREEQC version 3: a computer program for speciation, batch-reaction, one-dimensional transport, and inverse geochemical calculations. US Geological Survey Techniques and Methods, book 6, chap. A43, 497 p.; 2013.

(5) SNC-Lavalin Inc Mount Polley Mining Corporation post-event environmental impact assessment report, Appendix A: Hydrotechnical and geomorphological assessment, 621717; 2015.

(6) Byrne, P.; Runkel, R. L.; Walton-Day, K. Synoptic sampling and principal components analysis to identify sources of water and metals to an acid mine drainage stream. *Environ. Sci. Pollut. Res.* **2017** *24*, 17220-17240.

(7) Mayes, W. M.; Jarvis, A. P.; Burke, I. T.; Walton, M.; Feigl, V.; Klebercz, O.; Gruiz, K. Dispersal and attenuation of trace contaminants downstream of the Ajka bauxite residue (red mud) depository failure, Hungary. *Environ. Sci. Technol*. **2011** *45*, 5147-5155.